Effect of Molecular Conformations on the Adsorption Behavior of Gold-Binding Peptides

Marketa Hnilova,[†] Ersin Emre Oren,[†] Urartu O. S. Seker,[†,‡] Brandon R. Wilson,[†] Sebastiano Collino,[§] John S. Evans,[§] Candan Tamerler,[†,‡] and Mehmet Sarikaya*,[†]

Materials Science and Engineering, University of Washington, Seattle, Washington 98195, Molecular Biology and Genetics, Istanbul Technical University, Istanbul 34469, Turkey, and Laboratory for Chemical Physics, New York University, New York, New York 10010

Received May 12, 2008. Revised Manuscript Received July 7, 2008

Despite extensive recent reports on combinatorially selected inorganic-binding peptides and their bionanotechnological utility as synthesizers and molecular linkers, there is still only limited knowledge about the molecular mechanisms of peptide binding to solid surfaces. There is, therefore, much work that needs to be carried out in terms of both the fundamentals of solid-binding kinetics of peptides and the effects of peptide primary and secondary structures on their recognition and binding to solid materials. Here we discuss the effects of constraints imposed on FliTrx-selected gold-binding peptide molecular structures upon their quantitative gold-binding affinity. We first selected two novel gold-binding peptide (AuBP) sequences using a FliTrx random peptide display library. These were, then, synthesized in two different forms: cyclic (*c*), reproducing the original FliTrx gold-binding sequence as displayed on bacterial cells, and linear (*l*) dodecapeptide gold-binding sequences. All four gold-binding peptides were then analyzed for their adsorption behavior using surface plasmon resonance spectroscopy. The peptides exhibit a range of binding affinities to and adsorption kinetics on gold surfaces, with the equilibrium constant, K_{eq}, varying from 2.5×10^6 to 13.5×10^6 M^{-1}. Both circular dichroism and molecular mechanics/energy minimization studies reveal that each of the four peptides has various degrees of random coil and polyproline type II molecular conformations in solution. We found that AuBP1 retained its molecular conformation in both the *c*- and *l*-forms, and this is reflected in having similar adsorption behavior. On the other hand, the *c*- and *l*-forms of AuBP2 have different molecular structures, leading to differences in their gold-binding affinities.

Introduction

The utility of polypeptides in practical engineering has become common in recent years because of the development or adaptation of protocols and procedures from molecular biology and genetics that allow selection, design, and tailoring of these versatile biomolecules as molecular building blocks. In biology, proteins control the fabrication and assembly of inorganic structures in the form of hard tissues with myriad different functionalities, such as mechanical, magnetic, and optical.[1−4] Traditionally, large proteins have been used in engineering, mostly to increase the biocompatibility of implants and surface coating and make molecular scaffolds for use in tissue engineering. More recently, hybrid materials composed of noble-metal nanostructures functionalized with protein receptor molecules (e.g., antibodies and enzymes) have been of interest for developing novel chemo- and biosensors.[5−10] Ideally, the receptor coupling on the inorganic surface should be highly specific, highly ordered, reversible, and friendly to receptor molecules. Current inorganic surface coupling approaches are based on the creation of various self-assembled monolayer (SAM) linkages on metal inorganic surfaces, commonly using thiol or silane chemistry.[11,12] However, the SAM−surface interactions are nonspecific; e.g., thiols bind to any noble metal—gold, silver, or platinum—more or less equally likely.[11,13−15] An exciting alternative to chemical coupling may be the use of combinatorially selected inorganic-binding peptides as molecular linkers and assemblers.[1,3,16] In principle, in addition to the specific recognition of inorganic surfaces, combinatorially selected inorganic-binding peptides are robust and can be genetically engineered or modified to tailor their functionalities such as synthesizing, binding, erecting, and linking of inorganic nanostructures.[1,3]

Phage display[17] and cell surface display[18,19] have become the major in vivo techniques for the selection of material-specific peptides, generally called genetically engineered peptides for inorganics (GEPI).[1,20−23] Recently, peptide sequences specific

* To whom correspondence should be addressed. Phone: (206) 543-0724. Fax: (206) 543-3100. E-mail: sarikaya@u.washington.edu.
† University of Washington.
‡ Istanbul Technical University.
§ New York University.

(1) Sarikaya, M.; Tamerler, C.; Jen, A. K. Y.; Schulten, K.; Baenyx, F. *Nat. Mater.* **2003**, *2*, 577–85.
(2) Stupp, S. I.; Braun, P. V. *Science* **1997**, *277*, 1242–48.
(3) Sarikaya, M. *Proc. Natl. Acad. Sci. U.S.A.* **1999**, *25*, 14183–85.
(4) Seeman, N. C.; Belcher, A. M. *Proc. Natl. Acad. Sci. U.S.A.* **2002**, *99*, 6451–55.
(5) Haes, A. J.; Van Duyne, R. P. *J. Am. Chem. Soc.* **2002**, *124*, 10596–604.
(6) Haes, A. J.; Van Duyne, R. P. *Anal. Bioanal. Chem.* **2004**, *379*, 920–30.
(7) Haes, A. J.; Hall, W. P.; Chang, L.; Klein, W. L.; Van Duyne, R. P. *Nano Lett.* **2004**, *4*, 1029–1034.
(8) Haes, A. J.; Chang, L.; Klein, W. L.; Van Duyne, R. P. *J. Am. Chem. Soc.* **2005**, *127*, 2264–2271.
(9) Endo, T.; Yamamura, S.; Nagatani, N.; Morita, Y.; Takamura, Y.; Tamiya, E. *Sci. Technol. Adv. Mater.* **2005**, *6*, 491–500.
(10) Willets, K. A.; Van Duyne, R. P. *Annu. Rev. Phys. Chem.* **2007**, *58*, 267–97.
(11) Porter, M. D.; Bright, T. B.; Allara, D. L.; Chidsey, E. D. *J. Am. Chem. Soc.* **1987**, *109*, 3559–68.
(12) Laibinis, P. E.; Whitesides, G. M.; Allara, D. L.; Tao, Y. T.; Parikh, A. N.; Nuzzo, R. G. *J. Am. Chem. Soc.* **1991**, *113*, 7152–67.
(13) Fenter, P.; Eisenberger, P.; Li, J.; Camillone, N.; Bernasek, S.; Scoles, G.; Ramanarayaanan, T. A.; Liang, K. S. *Langmuir* **1991**, *7*, 2013–16.
(14) Li, Z.; Chang, S. C.; Williams, R. S. *Langmuir* **2003**, *19*, 6744–49.
(15) Love, J. C.; Estroff, L. A.; Kriebel, J. K.; Nuzzo, R. G.; Whitesides, G. M. *Chem. Rev.* **2005**, *105*, 1103–169.
(16) Krauland, E. M.; Peele, B. R.; Wittrup, K. D.; Belcher, A. M. *Biotechnol. Bioeng.* **2007**, *97*, 1009–20.
(17) Smith, G. P. *Science* **1985**, *228*, 1315–17.
(18) Brown, S. *Proc. Natl. Acad. Sci. U.S.A.* **1992**, *89*, 8651–55.
(19) Boder, E. T.; Wittrup, K. D. *Nat. Biotechnol.* **1997**, *15*, 553–57.
(20) Tamerler, C.; Oren, E. E.; Duman, M.; Venkatasubramanian, E.; Sarikaya, M. *Langmuir* **2006**, *22*, 7712–7718.

10.1021/la801468c CCC: $40.75
Published on Web 10/08/2008

for platinum, quartz, cuprous oxide, and hydroxyapatite, as well as many other materials and minerals, have been identified and characterized with regard to binding kinetics, affinities, and molecular structure.[24−27] Despite these most recent studies, there is still a need for detailed and quantitative data to address the molecular mechanisms that facilitate material-selective peptide binding on solid surfaces. The contribution of peptide primary and secondary structures most likely impacts the recognition and binding to solid materials, and this information is essential for future peptide engineering, peptide design, and robust utility of these novel small biomolecules, either alone or as a genetically fused part of a larger protein molecular construct, e.g., an enzyme.

Recently, a FliTrx bacterial expression system[28] was used to select peptide sequences directed against cuprous and zinc oxide substrates[29] and as a scaffold for various metal nanoparticle self-assemblies[30] and formations.[31] The FliTrx bacterial system uses the engineered extracellular flagellar protein (flagellin) to interact with solid substrates. The main feature of FliTrx peptide libraries is that random peptides are inserted as fusions within the thioredoxin active-site loop,[32] which is itself inserted into the dispensable region of the flagellin gene, as opposed to the N-terminal location of fusions made to coat proteins in phage display techniques. Thus, random peptides are displayed on the surface of bacteria within the structural context of the thioredoxin active-site loop, having both their N- and C- termini anchored by the rigid and stable tertiary structure of thioredoxin itself. Recently, structural constraints of FliTrx-selected cuprous oxide binding peptide have been discussed within the structural context of the DNA-binding fusion protein TraI.[27] It was shown that the presence of the disulfide-bonded loop of the Cu_2O sequence in TraI fusion protein was essential to mediate the adhesion and the reduction of this disulfide bond, completely abolishing the binding of the engineered TraI fusion protein to the Cu_2O surface.[27] However, the fundamentals of binding of such a disulfide-constrained peptide alone, i.e., without being in the context of other proteins (e.g., thioredoxin or TraI), and the effect of constraining on a peptide affinity to inorganics remain unknown.

To address the question of how the peptide molecular structure affects its function, i.e., solid binding, in this work, we discuss the effects of constraints imposed on FliTrx-selected gold-binding peptides. Here we use the selected peptides as stand-alone units, i.e., outside of the thioredoxin, to quantify their metal-binding affinity. Two identified gold-binding peptide (AuBP) sequences, AuBP1 (WAGAKRLVLRRE) and AuBP2 (WALRRSIRRQSY), were synthesized in two different forms: 18-aa Cys−Cys constrained loops, called cyclic (*c*), to mimic the original FliTrx displayed peptide conformations, and an open dodecapeptide version, called linear (*l*). Using surface plasmon resonance (SPR), circular dichroism (CD), and molecular modeling studies, we analyzed the effects of molecular conformations on peptide adsorption on the gold surface. We found that the cyclic versions of AuBPs have mainly random coil structures; however; the linear versions of AuBPs also have some degree of polyproline type II (PPII) rigid structures in addition to the random coil structures. The percentage of PPII structure in *l*-AuBP2 is greater than that in *l*-AuBP1, and thus, the structural differences between the *l*- and *c*-versions of AuBP2 are much bigger than the structural differences between the *l*- and *c*-versions of AuBP1. When the binding activities of the cyclic and linear versions of the same sequences were compared with each other, we observed that the change in the binding activity is directly related to molecular structural changes: *c*- and *l*-AuBP1 have comparable binding affinities and molecular structures; on the other hand, *c*- and *l*-AuBP2 have differences in their binding affinities and molecular structures.

Materials and Methods

Selection of Bacterial Gold-Binding Peptides. The AuBPs were selected from a FliTrx random peptide display library[28] (Invitrogen). Clean and 99.9% pure polycrystalline Au foils (Goodfellow Corp.) were used as a target in novel inorganic-binding peptide selection. Five selection rounds were applied in the panning experiment for gold-binding clone enrichment[29] (see the Supporting Information).

Calculation of the Expected and Observed Amino Acid Frequency in the FliTrx Library. We calculated the expected frequency of occurrence for each amino acid and for the STOP codon in the original naïve FliTrx library on the basis of published library construction parameters:[28] randomized dodecapeptides were coded by synthetic nucleotide triplets synthesized as $(XNN)_{12}$, where N was any nucleotide and X was a nucleotide with a deliberately biased ratio G:A:C:T of 7:7:7:3 (Supporting Information, Tables S1 and S2). We also generated the "observed" frequency of occurrence for all 20 amino acids in the original FliTrx library by randomly selecting and sequencing 92 clones from the unpanned FliTrx library. The calculated expected and observed amino acid frequencies, *P*, together with the probability of having at least one specific amino acid, P*, in a dodecapeptide are given in the Supporting Information (Table S3).

Chemical Synthesis of Gold-Binding Peptides. Gold-binding peptides *c*-AuBP1 (MW 1968.3, CGPWAGAKRLVLRREGPC), *l*-AuBP1 (MW 1454.7, WAGAKRLVLRRE), *c*-AuBP2 (MW 2106.4, CGPWALRRSIRRQSYGPC), and *l*-AuBP2 (MW 1591.8, WALRRSIRRQSY) were commercially synthesized using standard Fmoc solid-phase peptide synthesis techniques and purified using C-18 reversed-phase liquid chromatography (RP-HPLC) to a purity >95% (Bio-Peptide Co.).

SPR Experiments. SPR measurements were made with a four-channel instrument (Kretschmann configuration) developed by the Radio Engineering Institute, Czech Republic.[25] It was equipped with a polychromatic light source (Ocean Optics LS1): light from the source was connected to the detector by fiber optic cables. The instrument can detect changes at a level of 0.0001 refractive index unit and is temperature controlled (10−55 °C). Buffer and peptide solutions were degassed to avoid bubbles in the flow cell. First, a phosphate buffer solution (1:3 mixture of 10 mM KH_2PO_4, 10 mM K_2HPO_4, and 100 mM KCl) was flowed over the surface until a stable baseline signal was established. Then peptide solutions made by dissolving peptides in phosphate buffer at concentrations between 0.23 and 2 μM were flowed over the surface, and adsorption was monitored. After the surface coverage reached or neared equilibrium, the phosphate buffer solution was flowed again, and desorption of the peptide was monitored. The system was then cleaned using a 1% SDS + 0.1 M NaOH solution, followed by a 0.1 M HCl solution and, finally, by DI water.

(21) Whaley, R. S.; English, D. S.; Hu, L. E.; Barbara, F. P.; Belcher, M. A. *Nature* **2002**, *405*, 665–68.
(22) Naik, R. R.; Stringer, S. J.; Agarwal, G.; Jones, S. E.; Stone, M. O. *Nat. Mater.* **2002**, *1*, 169–71.
(23) Nam, K. I.; Kim, D. W.; Yoo, P. J.; Chiang, C. Y.; Meethong, N.; Hammond, P. T.; Chiang, Y. M.; Belcher, A. M. *Science* **2006**, *312*, 885–89.
(24) Oren, E. E.; Tamerler, C.; Sahin, D.; Hnilova, M.; Seker, U. O. S.; Sarikaya, M.; Samudrala, R. *Bioinformatics* **2007**, *23*, 2816–2822.
(25) Seker, U. O. S.; Wilson, B.; Dincer, I. S.; Kim, I. W.; Oren, E. E.; Evans, J. S.; Tamerler, C.; Sarikaya, M. *Langmuir* **2007**, *23*, 7895–7900.
(26) Gungormus, M.; Fong, H.; Kim, I. W.; Evans, J. S.; Tamerler, C.; Sarikaya, M. *Biomacromolecules* **2008**, *9*, 966–973.
(27) Choe, W.-S.; Sastry, M. S. R.; Thai, C. K.; Dai, H.; Schwartz, D. T.; Baneyx, F. *Langmuir* **2007**, *23*, 11347–350.
(28) Lu, Z.; Murray, K. S.; Van Cleave, V.; LaVallie, E. R.; Stahl, M. L.; McCoy, J. M. *Bio/Technology* **1995**, *13*, 366–72.
(29) Thai, C. K.; Dai, H.; Sastry, M. S. R.; Sarikaya, M.; Schwartz, D. T.; Baneyx, F. *Biotechnol. Bioeng.* **2004**, *87*, 129–137.
(30) Kumara, M. T.; Tripp, B. C.; Muralidharan, S. *Chem. Mater.* **2007**, *19*, 2056–64.
(31) Kumara, M. T.; Srividya, N.; Muralidharan, S.; Tripp, B. C. *Nano Lett.* **2006**, *6*, 2121–29.
(32) LaVallie, E. R.; DiBlasio, E. E.; Kovacic, S.; Grant, K. L.; Schendel, P. F.; McCoy, J. M. *Biotechnology* **1993**, *11*, 187.

CD Experiments. Lyophilized synthetic peptides were dissolved in distilled DI water to create stock solutions which were then diluted to final peptide concentrations of 2, 4, 8, 12, 20, and 25 μM in 100 μM Tris−HCl, all at pH 7.5. CD spectra were recorded on an AVIV 60 CD spectrometer, running 60DS software, version 4.1t. The CD spectrometer was calibrated with D-10-camphorsulfonic acid. Wavelength scans were conducted from 185 to 260 nm with buffer and solvent background subtraction.[33,34] For each spectrum, three scans were averaged using a 1 nm bandwidth and a scanning rate of 0.5 nm/s. The mean residue ellipticity (θ_M) is expressed in deg cm^2 dmol^{-1}.

Molecular Modeling Studies. To model the linear and cyclic versions of AuBPs, we built linear forms and generated cyclic versions via the addition of cysteine residues at both the N- and C-termini, followed by covalent modification of the Cys−Cys pairs to create a disulfide bridge. The energy minimization of these peptides was carried out under implicit solvent conditions using the conformational analysis programs in HyperChem's molecular modeling software (Hyperchem 7.5). The conformational search module finds the minimum-energy structures by varying the chosen dihedral angles. To perform energy minimization, the program changes dihedral angles randomly and creates new initial structures. In each round of energy minimization, unique low-energy conformations are stored, and high-energy and duplicate structures are discarded. Using the conformational search module, we found 1000 different local minima on the potential energy surface, and we chose the lowest one as the global minimum or the lowest energy conformation.[35,36] Then the lowest energy conformations were solvated with TIP3P water explicitly, and finally the overall system was energy minimized using the Polak−Ribiere conjugate gradient method until convergence of the gradient (0.01 kJ/mol) was reached using the CHARMM 27 force field.[37] From the final structures of *c*- and *l*-AuBPs, we calculated the root-mean-square deviation (rmsd) values for both the backbone atoms and all atoms of the integral sequences by using HyperChem's molecular modeling software (Hyperchem 7.5).

Results and Discussion

Clone Selection and Binding Characterization. The main feature of the FliTrx library (Invitrogen) is that the randomized peptides are displayed in a well-defined structural context due to the thioredoxin active-site loop,[28] as opposed to M13 phage libraries (New England Biolabs) that display peptides as the N-terminal fusion on the minor PIII coat protein. The next advantage of the FliTrx cell surface display library system over the phage display library is its greater efficiency in generating peptide sequences, due to the fact that it does not need a second host organism to amplify and replicate genomic sequences. Thus, for the gold-binding biopanning selection we chose the FliTrx peptide library for its shorter generation times and more simplified amplification/panning protocol. This is in spite of the fact that the FliTrx library diversity of randomized sequences (1.77×10^8 random dodecamer sequences) is an order of magnitude lower than the diversity of phage peptide libraries (2.7×10^9 random dodecamer sequences). After 5 successive rounds of biopanning selection to enrich for strong gold binders, 50 randomly selected clones were sequenced to determine the amino acid composition of the randomized insertions (Supporting Information). These 50 clones were further analyzed for binding affinities via fluorescence microscopy to gain insight into the relationship between amino acid composition and strength of binding. The

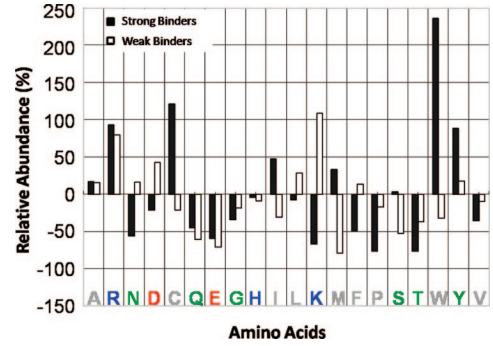

Figure 1. Relative abundance of amino acids in strong- and weak-binding groups of gold-binding peptides. The residues are colored as basic = blue, acidic = red, hydrogen-bonding donor/acceptor = green, and nonpolar = grey. The amino acid distribution of the original FliTrx peptide library is shown in the Supporting Information (Table S3).

Table 1. MW, pI, and Net Charge of Fmoc-Synthesized Gold-Binding Peptides Computed Using ProtParam (www.expasy.org)

name	sequence	MW	pI	charge
l-AuBP1	WAGAKRLVLRRE	1454.7	11.7	+3
c-AuBP1	CGPWAGAKRLVLRREGPC	1967.3	9.7	+3
l-AuBP2	WALRRSIRRQSY	1591.8	12	+4
c-AuBP2	CGPWALRRSIRRQSYGPC	2106.4	10.7	+4

bound cells expressing gold-binding sequences were visualized as fairly uniformly distributed bright rods on a dark background, as opposed to GI826 plasmid free control cells which did not adhere to the gold substrate (Supporting Information, Figure S1). The binding affinity of selected gold-binding clones was estimated by enumerating adhered cells in three random regions in duplicate experiments; this led to the identification of three binding groups as strong, moderate, and weak (see the Supporting Information, Figure S1).

The gold-binding sequences did not converge toward a consensus sequence even after five biopanning rounds. Therefore, we compared the observed amino acid composition among strong, moderate, and weak binder groups of selected gold-binding sequences with the naïve (unpanned) library (Supporting Information, Table S3) to calculate the relative abundances of amino acids among them. We found that Arg, Cys, Trp, and Tyr were overexpressed and Asn, Lys, Pro, and Thr underexpressed among our selected strong binder sequences (Figure 1). The overexpression of Cys would be expected since the present thiol group has an affinity to gold surfaces.[11,15] Also overexpression of Tyr is in agreement with the literature since peptides containing hydroxyl-rich residues have been reported to have high affinity to the gold lattice.[1,20,23,38] Arg was overexpressed not only among the strong gold-binding peptides but also among the weak-binding peptides as well. Furthermore, the Arg overexpression was also featured in peptide sequences that were selected against other materials (e.g., cuprous oxide and zinc oxide)[29] using the same cell surface display technique. Thus, the role of Arg overexpression in selected peptide sequences is still not clear.

For quantitative studies of the absorption kinetics of our novel gold-binding peptides to gold surfaces, we chose to use the two integral gold-binding peptide sequences (termed AuBP1 and AuBP2, Table 1) that exhibited the highest affinity to gold when displayed on bacterial cells as FliTrx fusion proteins (Supporting Information, Figure S1). These integral AuBPs contain neither individual Cys nor individual His amino acids, which are known

(33) Collino, S.; Kim, I. W.; Evans, J. S. *Cryst. Growth Des.* **2006**, *6*, 839–842.
(34) Kulp, J. L.; Minamisawa, T.; Shiba, K.; Evans, J. S. *Langmuir* **2007**, *23*, 3857–3863.
(35) Cubellis, M. V.; Caillez, F.; Blundell, T. L.; Lovell, S. C. *Proteins Struct. Funct. Bioinf.* **2005**, *58*, 880–892.
(36) Oren, E. E.; Tamerler, C.; Sarikaya, M. *Nano Lett.* **2005**, *5*, 415–419.
(37) MacKerrell, A. D., Jr.; Bashford, D.; Bellott, M.; Dunbrack, R. L., Jr.; Evanseck, J. D.; Field, M. J.; Fischer, S.; Gao, J.; Guo, H.; Ha, S. *J. Phys. Chem. B* **1998**, *102*, 3586–3616.
(38) Huang, Y.; Chiang, C.-Y.; Lee, S. K.; Gao, Y.; Hu, E. L.; Yoreo, J. D.; Belcher, A. M. *Nano Lett.* **2005**, *5*, 1429–34.

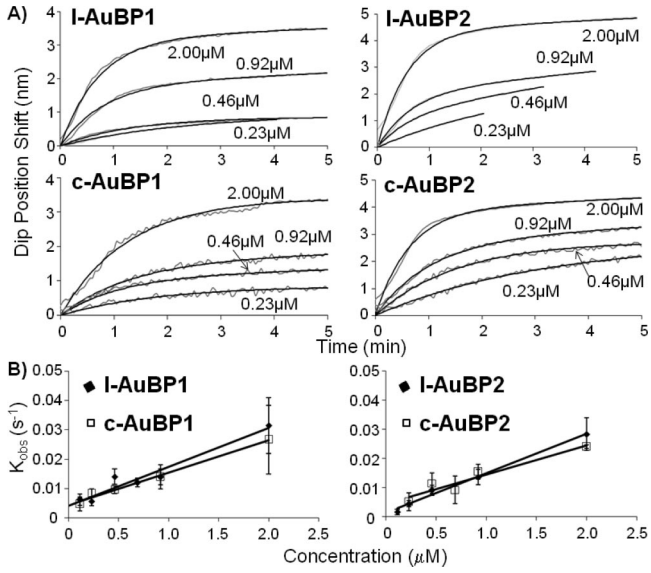

Figure 2. (A) Adsorption isotherms for linear and constraint forms of AuBP1 and AuBP2, obtained by SPR, at different concentrations. The gray lines represent experimental data points, and the black lines are Langmuir model fits. (B) Observed rate coefficients (K_{obs}) plotted as a function of the peptide concentration. Linear regression was used to calculate the adsorption (k_a) and desorption (k_d) rates.

to form stable metal−sulfur bonds[11,15] or to bind to transition-metal ions.[1,39,40] The lack of these individual amino acids in the selected AuBPs eliminates obvious well-known metal-binding mechanisms by which peptides can attach to our metal surfaces and indicates a novel gold-binding mechanism.

The FliTrx-selected gold-binding sequences were originally displayed on bacterial cells as cyclic Cys−Cys disulfide loops.[28] Here, to determine how this restricted conformation of FliTrx-selected AuPBs affects peptide functionality on gold, we synthesized both AuBP sequences in two different versions: original constrained and respective linear. The constrained gold-binding versions (*c*-AuBP1, *c*-AuBP2) were synthesized by adding CPG at the N-terminus and GPC at the C-terminus of each sequence (total length 18 aa) to reproduce the original loop displayed by the FliTrx system. The linear versions of *l*-AuBP1 and *l*-AuBP2 were, likewise, synthesized as the dodecapeptides, i.e., minus the N- and C-terminal tripeptide fragments.

Gold−Peptide Adsorption Kinetics and Thermodynamics. Raw kinetic data from SPR tests were fitted by least-squares regression to a 1:1 Langmuir adsorption model, per

$$\theta(t - t_0) = \theta_\infty[1 - \exp(-k_{obs}(t - t_0))] \quad (1)$$

where θ_∞ is the equilibrium surface coverage and $k_{obs} = k_a C + k_d$. We calculated the adsorption rate (k_a) and the desorption rate (k_d) by determining k_{obs} at several concentrations. From these kinetic constants the equilibrium constant (K_{eq}) and free energy change of adsorption (ΔG) were also calculated.[25,41] The fits and resulting kinetic constants (K_{eq}, k_a, k_d, and ΔG) are shown in Figure 2 and Table 2, respectively.

The binding characteristics of all tested AuBPs are similar, except for the constrained form of *c*-AuBP2 (Table 2). The major difference in the binding kinetics of *c*-AuBP2 is a significantly lower desorption rate than the desorption rate of the other AuBPs. The difference in the desorption rate is reflected in the equilibrium constants and ΔG. Thus, this lower desorption rate leads to higher K_{eq} and ΔG values for *c*-AuBP2 versus other AuBPs. The SPR results also show that the novel FliTrx-selected *l*-AuBP1, *c*-AuBP1, and *l*-AuBP2 have almost the same binding properties as other previously selected gold-binding peptides, namely, 1r-GBP1 (MHGKTQATSGTIQS).[1,20] *c*-AuBP2 has an even significantly lower binding energy (-9.7 ± 0.1 kcal/mol) compared to 1r-GBP1 (-8.4 ± 0.1 kcal/mol). This 1.3 kcal/mol difference represents an order of magnitude higher equilibrium constant for *c*-AuBP2 than for 1-GBP1. The fundamental difference in solid-binding between the two peptides is the desorption rate (k_d), which is lower in *c*-AuBP2. All adsorption kinetics of the AuBPs were measured in water-based solvents, providing more biology-friendly conditions, desirable for most biotechnology and medical applications. Thus, it is clear that these combinatorially selected AuBPs could be a viable alternative to many conventionally used thiol-based systems as a molecular linker in a wide range of applications.

Conformational Properties of Cyclic and Linear AuBP Sequences. Conformational instability is a common feature of several proteins involved in mineral formation/modification and is believed to be a driving force for polypeptide-mediated crystal growth and regulation, where interaction with mineral surfaces and/or ion clusters induces polypeptide folding or internal stabilization.[26,33] We have also demonstrated that conformationally labile structures exist within phage display peptide sequences directed against platinum metal and hydroxyapatite.[25,26] To determine whether this phenomenon exists in our AuBP sequences, we investigated the conformation of the two AuBPs with two different forms in solution using CD spectrometry (Figure 3). Although NMR methods are more quantitative, they are not necessarily more informative for short, conformationally labile peptides such as the 12-aa and 18-aa AuBP series. CD spectra for all four peptides feature a (−) $\pi-\pi^*$ transition band centered between 195 and 201 nm, which is consistent with the presence of a random coil (RC) conformation in equilibrium with other secondary structures.[25,34,35,42,43] Thus, all AuBP polypeptides share the common traits of the RC structure, which is conformationally unstable. Presumably, the RC conformation somehow enables AuBP sequences to interact with Au surfaces, but how this is accomplished is not yet known.

In addition to the RC-associated ellipticity band, *l*-AuBP1 and *l*-AuBP2 also have a second (+) ellipticity band (n−π^* transition) centered near 220 nm (Figure 3) which corresponds to extended helical polyproline type II (PPII) secondary structures.[35,43] This ellipticity band is most intense in *l*-AuBP2, which indicates that the percentage of PPII structure in *l*-AuBP2 is greater than that in *l*-AuBP1. The PPII conformation is also affiliated with polyelectrolyte sequence blocks like those found in AuBP1 and AuBP2 (i.e., −KR− and −RR−, Table 1), and the PPII structure is often found in protein sequences which are involved in intermolecular interactions.[35,43] Note that this PPII-associated ellipticity band is not observed for either *c*-AuBP1 or *c*-AuBP2, indicating that, although the integral sequences are the same, the loop acts as a constraint which prevents the formation of the extended PPII helix in *c*-AuBP1 and *c*-AuBP2. Thus, in addition to RC, the linear versions of AuBP1 and AuBP2 possess some percentage of extended helical PPII structure which facilitates side chain accessibility and display for Au interactions. The significance of the PPII structure in these sequences is currently being investigated.

(39) Slocik, J. M.; Wright, D. W. *Biomacromolecules* **2003**, *4*, 1135–41.
(40) Slocik, J. M.; Moore, J. T.; Wright, D. W. *Nano Lett.* **2002**, *2*, 169.
(41) Tamerler, C.; Duman, M.; Oren, E. E.; Gungormus, M.; Xiong, X.; Kacar, T.; Parvitz, B. A.; Sarikaya, M. *Small* **2006**, *2*, 1372–78.
(42) Evans, J. S. *Curr. Opin. Colloid Interface Sci.* **2003**, *8*, 48–54.
(43) Chellgren, B. W.; Creamer, T. P. *Biochemistry* **2004**, *43*, 5864–5869.

Table 2. Adsorption Rate (k_a), Desorption Rate (k_d), Equilibrium Coefficient (K_{eq}), and Free Energy for Linear (*l*) and Constrained (*c*) Gold-Binding Peptides

peptide	$K_{eq} \times 10^6$ (M^{-1})	$k_a \times 10^5$ (M^{-1} s^{-1})	$k_d \times 10^{-4}$(s^{-1})	ΔG_{ads} (kcal/mol)
l-AuBP1	3.24 ± 1.31	1.32 ± 0.21	41 ± 8	−8.9 ± 0.2
c-AuBP1	2.51 ± 0.50	1.10 ± 0.22	44 ± 2	−8.7 ± 0.1
l-AuBP2	2.34 ± 0.34	1.00 ± 0.03	43 ± 5	−8.7 ± 0.1
c-AuBP2	13.50 ± 3.00	1.35 ± 0.12	10 ± 2	−9.7 ± 0.2

Molecular mechanics/energy minimization studies suggest plausible 3-D models of the AuBPs (Figure 4). In all cases, the presence of an unfolded structure leads to creation of accessible side chain regions, presumably important for peptide interaction at the gold interfaces. There are some interesting primary sequence features. (1) Cationic −KR− and −RR− sequence diads that give rise to positively charged motifs are present at the surface of each sequence. However, these diads are positioned closer together (near the middle) in the AuBP2 sequence series, but in the AuBP1 sequence series they are separated from each other

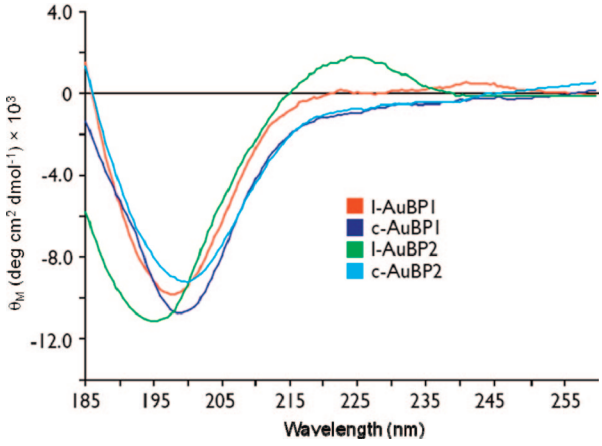

Figure 3. CD spectra of AuBPs in 100 μM Tris−HCl, pH 7.5.

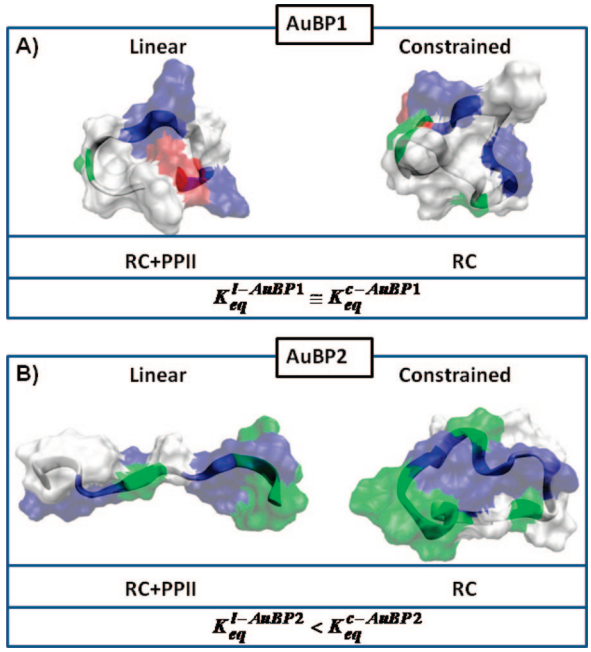

Figure 4. Overlapped ribbon and transparent surface models of the predicted structures of the *l*- and *c*-versions of AuBP1 (A) and AuBP2 (B). Both CD spectra and molecular dynamics analyses indicate that the percentage of PPII structure in *l*-AuBP2 is greater than that in *l*-AuBP1. RC = random coil, and PPII = polyproline type II structure (see the text).

Table 3. All-Atom and Backbone rmsd between the *c*- and *l*-Versions of Gold-Binding Peptides

	AuBP1 *l*−*c* (Å)	AuBP2 *l*−*c* (Å)
all-atom rmsd	4.7	7.5
backbone rmsd	2.3	5.2

by an intervening −LVL− hydrophobic motif. (2) Hydrogen-bonding donor/acceptor amino acids Gln, Ser, and Tyr, which exist in sequence clusters within biomineralization-associated peptides,[26,33,34,42] are also found as a triplet sequence cluster at the C-terminal end of AuBP2 but are absent in AuBP1. (3) Only the AuBP1 peptide has an anionic Glu residue at the C-terminal. (4) The highest affinity binder, *c*-AuBP2, also has the largest molecular volume. Thus, the structural features of the AuBP peptide series relate to their functional properties as follows. Each peptide has some degree of RC structure, and there is some degree of PPII structure in the linear versions of AuBP. Collectively, these structural features promote unfolded, conformationally labile peptides that enhance their adaptability of interfacial features that exist on gold surfaces (e.g., surface topology, interfacially bound water layers). This is probably why the AuBPs bind to gold with high binding affinities.

The conformational and molecular dynamic properties of these peptides are hypothesized to modulate the binding affinities by altering the side chain accessibility or positioning with respect to the target surface.[25] Our findings are summarized in Figure 4. Conformational analysis of both the linear and constrained versions of AuBP2 shows a significant difference in the secondary structures adopted by *l*-AuBP2 (RC with great degree of extended PPII) compared to *c*-AuBP2 (collapsed RC). To assess the structural differences between the *c*- and *l*-versions of AuBP1 and AuBP2, we calculated both the all-atom rmsd and the backbone rmsd between the two versions of AuBPs (Table 3). The higher the rmsd the more different the two structures. The significantly different adapted secondary structures of AuBP2 peptides (5.2 Å backbone rmsd) may explain the binding affinity decrease for the linear version of the originally constrained AuBP2 ($K_{eq} = 2.34 \times 10^6$ and 13.5×10^6 M^{-1} for *l*-AuBP2 and *c*-AuBP2, respectively). On the other hand, the similar adsorption behavior of the linear and constrained versions of AuBP1 (e.g., $K_{eq} = 3.24 \times 10^6$ and 2.51×10^6 M^{-1} for *l*-AuBP1 and *c*-AuBP1, respectively) evidenced by SPR analysis is probably due to the favorable comparable secondary structures (2.3 Å backbone rmsd) adapted by constrained (collapsed RC) and linear (collapsed RC with low degree of extended PPII) AuBP1 (Figure 4). These observations are in agreement with our earlier findings obtained with the selected M13 9-aa cyclic version and its 7-aa synthetic linear version of the Pt-binding sequences,[25] where the conformational state had an impact on the peptide binding affinity to the Pt surface.

Conclusion

Most studies on the adsorption behavior of combinatorially selected inorganic-binding peptides onto solids have focused mainly on their amino acid compositions.[16,20−23,29,38,41] Only recently some studies addressed the peptide structural constraints on the adsorption behavior and affinity to solids.[25−27] The

understanding of quantitative peptide binding to solids is crucial from the points of both the fundamental understanding of the mechanism(s) of peptide binding to solids and their robust utilization in practical applications. It is well-known in protein engineering that the protein molecular architecture affects its function. Here, we hypothesized that the structure−function relationship also persists in peptide binding to inorganic materials. To assess the hypothesis, we used two gold-binding peptides that were originally selected in a cyclic form, i.e., a constraint architecture, and compared their adsorption and conformational behaviors to those of their linear, free forms using respectively SPR and CD spectroscopy and computational modeling. The SPR analysis showed that both the linear and cyclic forms of AuBPs have high affinities to gold (e.g., $\Delta G_{ads} \leq -8.7$ kcal/mol). We also found that both the linear and cyclic forms of AuBPs have random coil and PPII structures, which cooperatively promote unfolded, conformationally labile peptides that may enhance their adaptability to interfacial features that exist on gold surfaces. One would expect differences in the binding characteristics between the cyclic and linear forms as the structure may change. We found that AuBP2 has an order of magnitude higher affinity in the cyclic version than in the linear one. This difference is consistent with the observation of significant structural change in the molecular conformations of the cyclic and linear versions of AuBP2 in solution. On the other hand, the binding affinities of AuBP1 in the cyclic and linear forms are quite similar. In this case, we found that the molecular structures of this peptide in the two versions are similar, as we show both experimentally (CD) and via modeling. On the basis of all the evidence, we show that the peptide molecular conformation and its sequential amino acid content may be the key determinants that facilitate peptide selective binding on solid materials.

Acknowledgment. This work was mainly supported by the Genetically Engineered Materials Science & Engineering Center (GEMSEC) and NSF-MRSEC at the University of Washington. Partial support (C.T. and U.O.S.S.) was provided by the Turkish State Planning Organization via Advanced Technologies in Engineering. Portions of this work represent contribution number 43 from the Laboratory of Chemical Physics, New York University (J.S.E.).

Supporting Information Available: Details of the peptide selection-binding characterization and calculation of the AA composition of the FliTrx peptide library. This material is available free of charge via the Internet at http://pubs.acs.org.

LA801468C